Calculation of Intermolecular Interaction Energies by Direct Numerical Integration over Electron Densities. 2. An Improved Polarization Model and the Evaluation of Dispersion and Repulsion Energies

A. Gavezzotti

Dipartimento di Chimica Strutturale e Stereochimica inorganica, Università di Milano, via Venezian 21, 20133 Milano, Italy

Received: October 22, 2002; In Final Form: January 9, 2003

A procedure to adapt electron densities of isolated molecules for the evaluation of intermolecular energies, first introduced in paper 1 (Gavezzotti, A. *J. Phys. Chem. B* **2002**, *106*, 4145) is here improved for polarization energy and extended to dispersion and repulsion terms. Dispersion is evaluated from atomic polarizabilities distributed over the electron density, using an average ionization potential taken as the energy of the highest occupied molecular orbital, in a London-type inverse sixth-power formulation. Repulsion is evaluated from the overlap between electron densities. The method, called semiclassical density sums (SCDS), requires only four disposable numerical parameters and allows a complete evaluation of intermolecular interaction energies for a rather wide range of molecular systems. Calculations on molecular dimers, in comparison with results obtained by high-level quantum chemical methods, show that SCDS energies are quite reliable, at a fraction of the computational cost. The sublimation energies of many organic crystals are well reproduced by the corresponding calculated lattice energies, which include significant polarization contributions. The method allows a partitioning of intermolecular interactions over molecular pairs in crystals; this in turn allows for the first time a quantitative assessment of the relative importance of Coulombic, repulsion, and dispersion energies in the interaction between atom groups and in crystal packing in general, often contradicting some current views based on intuitive or even semiquantitative electrostatic models that do not include penetration terms.

I. Introduction

The development of conceptual procedures for the rationalization of the structure of crystalline solids has recently been a matter of considerable interest.[1,2] This goal is pursued both by experimentalists, synthetic solid-state chemists whose aim is the actual preparation of crystalline materials, and by theoreticians, whose aim is the generation of plausible crystal structures by computer. In one approach,[3,4] the chemistry of intermolecular interactions is handled with concepts such as shape or charge complementarity, or pattern recognition and reproduction, with an attempted extension of concepts and strategies borrowed from synthetic intramolecular chemistry. This approach relies on intuitive, qualitative links between a known intermolecular geometry and an unknown intermolecular potential; the attractive neologism "crystal engineering" applies.

A more robust strategy calls for the accurate calculation of intermolecular fields. Even so, there are indications that current atom−atom force fields are intrinsically unable to provide the accuracy required for a reliable energetic ranking of polymorphic structures.[5,6] We have proposed in paper 1[7] a new approach to this formidable problem, using free-molecule electron densities obtained by molecular orbital calculations; a satisfactory protocol for the calculation of Coulombic energies was described, with a first approach to the calculation of polarization energies. The present paper deals with an improvement of the polarization energy scheme and with the calculation of dispersion and repulsion energies. Total lattice energies can thus be estimated. The method is parametrized and validated by comparison with high-level ab initio quantum chemical calculations for dimers of small molecules and by reproduction of the sublimation enthalpies of a selection of organic crystals. Then, it is applied to the partitioning of total crystal energies into molecule-molecule contributions, revealing so far unknown detail of the energetic weaving of molecular crystals.

We call the new procedure semiclassical density sums (SCDS) method, because it stands upon the use of quantum mechanical results in formulas of classical electrostatics. It has a much more solid physical foundation and a much higher performance/parameter ratio than atom−atom force fields.

II. Revision of the Previous Model

A. General Layout. The molecular electron density is calculated[8] at the MP2/6-31G** level, on a grid with a standard step of 0.08 Å. For acetic acid, formamide, and benzene, symmetrized molecular models were used in the dimer calculations, whereas the uncorrected molecular conformations found in the crystal were used for the crystal calculations. Valence-only electron densities are used throughout. Each electron pixel has a density ρ_i, a volume V_i, and hence a charge $q_i = \rho_i V_i$. Super-pixels are then formed by condensing $n \times n \times n$ original pixels, with n being called the condensation level. When the original number of grid points is a multiple of n, the symmetry of the density cloud is better preserved. Super pixels whose charge is below a given threshold, q_{min}, are screened out. After extensive testing, the values $n = 4$ and $q_{min} = 10^{-6}$ electrons were chosen as the best compromise between accuracy and computing times. Some results for $n = 3$ will also be discussed. Appendix I should be consulted for some other minor details.

B. Coulombic Energies, E_{COUL}. As before,[7] these are calculated as summations over intermolecular pixel−pixel, pixel−nuclei, and nuclei−nuclei Coulombic terms. Extensive tests were carried out to check the adverse effects of discrete

10.1021/jp022288f CCC: $25.00
Published on Web 02/15/2003

TABLE 1: Atomic Polarizabilities and Atomic Radii

atom	α_{atom}/Å^3	atomic radius/Å[a]
C(aliphatic)	1.05	1.77
C(unsaturated)	1.30	1.77
O	0.80	1.58
N	0.88	1.64
H	0.39	1.10
Cl	2.30	1.76
S	3.00[b]	1.81
Ar	1.70	2.70

[a] From ref 39. [b] From ref 9c.

integration: in particular as concerns (i) nonsphericity or missed symmetry in atomic densities (because the density is represented as a set of cubes of finite size) and (ii) fortuitous exact overlap of pixels, resulting in zero or near-zero pixel−pixel distance. These factors may cause singularities or breakdown in the rotational invariance of calculated energies. All pixel−pixel distances below half the stepsize (0.16 or 0.12 Å for $n = 4$ or 3, respectively) were reset at 0.16 or 0.12 Å: we call these numbers the "collision avoidance" threshold.

C. Polarization Energies, E_{POL}. Calling ϵ_i the electric field exerted by surrounding molecules at pixel i, α_i the polarizability at pixel i, and μ_i the dipole induced at pixel i by that field, the linear polarization energy is

$$E_{POL,i} = -1/2\mu_i \epsilon_i = -1/2\alpha_i \epsilon_i^2 \quad (1)$$

The total field is the vector sum of fields generated by each pixel in all the surrounding molecules. As already pointed out in paper 1, the main defects of this scheme are (i) the uncertainty in the definition of the distributed polarizabilities, α_i, (ii) the divergence at very short distances between polarizing and polarized pixels, and (iii) the fact that the polarization is static, i.e., densities are not dynamically deformed by polarization. No simple solution to this last problem seems to be in sight, but improvements were devised for points i and ii.

To assign pixel polarizabilities, each pixel has to be first assigned to a particular atom in the molecule. In paper 1, pixels were assigned to the atom to whose nucleus they were closest; in the present, improved scheme, each pixel is assigned to the atom to which the distance is the smallest fraction of the atomic radius (see Table 1). Calling α_{atom} the atomic polarizability, and Z_{atom} the number of valence electrons in that atom, we then write

$$\alpha_i = (q_i/Z_{atom})\alpha_{atom} \quad (2)$$

An entirely new set of atomic polarizabilities were derived (Table 1) by partitioning experimental molecular polarizabilities, as collected from standard references,[9a,b] into atomic contributions. The additivity is excellent: over 41 molecules the least-squares fit gave $\alpha_{calc} = 0.985\ \alpha_{obs}$ ($R^2 = 0.998$). This new scheme is much simpler, but equally effective, than the old one; moreover, the sum of pixel polarizabilities is now equal to the total molecular polarizability, usually within 1%. The atomic polarizabilities in Table 1 are nonadjustable parameters in the formulation. Further subdivision of atomic polarizabilities into subspecies[9c] was considered premature, except for aliphatic and aromatic carbon.

Polarization contributions at very short separations pose a complex problem (sometimes called the polarization catastrophe[9d]). Ideally, one should use higher-order, nonlinear polarization coefficients, but that would be too complicated. We have instead preserved the linear polarization form, adding a damping scheme. Preliminary tests using a damping factor directly on single contributions in the summation for electric fields gave inconsistent results. Therefore, the damping factor was applied to the resulting field. A survey in a few molecular crystals revealed that fields at e pixels are mostly of the order of 10^{10} V m^{-1}, plus a small number in the $10^{10}-10^{13}$ V m^{-1} range, plus a very small number of even higher ones, especially in hydrogen-bonded crystals. These high-field contributions are physically unrealistic, resulting from fortuitous short distances in the overlapping density meshes, and cause severe ill-conditioning in the polarization energy sums. Pixel−pixel distances were subjected to the collision avoidance scheme (see in section II.B); then, the damped polarization energy at pixel i is

$$E_{POL,i} = -1/2\alpha_i[\epsilon_i d_i]^2 \text{ for } \epsilon < \epsilon_{max} \quad (3a)$$

$$d_i = \exp -(\epsilon_i/(\epsilon_{max} - \epsilon_i)) \quad (3b)$$

$$E_{POL,i} = 0 \text{ for } \epsilon > \epsilon_{max} \quad (3c)$$

The threshold value ϵ_{max} must be considered an adjustable empirical parameter in the formulation. It was set here at 200×10^{10} V m^{-1}. The total polarization energy at a molecule is the sum of polarization energies at each of its electron density pixels, as before[7]

$$E_{POL,TOT} = \sum E_{POL,i} \quad (4)$$

whereas the total polarization energy in an ensemble of molecules is the sum of all A...B and B....A polarization energies (in this respect, see Appendix I for an important consideration as regards lattice sums in crystals).

III. Dispersion Energies

The original London formulation for the dispersion energy between two molecules of polarizability α and ionization energy E_{ION} is[10]

$$E = -3/4(E_{ION}\alpha^2)/[(4\pi\epsilon^\circ)^2(R_{ij})^6] \quad (5)$$

In the present method, intermolecular dispersion energies are calculated as a sum of pixel−pixel terms in a London-type expression, involving the above-defined distributed polarizabilities (eq 2) and an overall ionization energy, E_{ION}. To avoid singularities due to very short pixel−pixel distances in an inverse sixth-power formula, each term in the sum is damped according to a literature function, $f(R)$, used in the calculation of dispersion energies by quantum mechanical methods.[11] The complete expression for a two-molecule A...B interaction is

$$E_{DISP,AB} = E_{ION}(-3/4)\sum\sum f(R)\alpha_i\alpha_j/[(4\pi\epsilon^\circ)^2(R_{ij})^6] \quad (6a)$$

$$f(R) = \exp[-(D/R_{ij} - 1)^2] \text{ for } R_{ij} < D \quad (6b)$$

$$f(R) = 1 \text{ for } R_{ij} > D \quad (6c)$$

D, the damping threshold distance, is an adjustable empirical parameter. Its order of magnitude in previous use[11] (however, in a different context) is of a few Å units; it was set here at 3.25 Å.

We use for E_{ION} the energy of the highest occupied molecular orbital

$$E_{ION} = -E_{HOMO} \quad (7)$$

This is again a nonadjustable parameter in the formulation, being directly and unequivocally obtained from the molecular orbital calculation. When two different molecules interact, E_{ION} is taken as the geometrical average of the two ionization potentials (although the arithmetic or harmonic mean could also have been considered; this point is deferred to further work on heterogeneous systems).

For a crystal, the total dispersion energy is a sum of two-body interactions

$$E_{DISP} = 1/2\sum\sum E_{DISP,AB} \tag{8}$$

where the factor 1/2 arises because of lattice sums (Appendix I).

IV. Repulsion Energies

The repulsion energy between molecules A and B is obtained[12] from the overlap between their electron densities, S_{AB}

$$E_{REP,AB} = K(S_{AB})^{\gamma} \tag{9}$$

$$S_{AB} = \sum\sum[\rho_i(A)\ \rho_j(B)]V \tag{10}$$

Equation 10, where the ρ's are the electron densities in two pixels and V is the pixel volume, is the discrete equivalent of the overlap integral.

For the calculation of S_{AB}, the original uncondensed electron density of each of the two molecules is rotated and translated according to the relative space orientation of the two molecules. The parallelepiped that contains the overlap zone is then scanned on a grid with a step equal to the average of the two original density steps, and a point by point integration is carried out using the summation in eq 10. The value of $\rho_i(A)$ or $\rho_j(B)$ at any current point in the space of the two original densities is evaluated by interpolation among the values at the eight corners of the cube-let that contains the current point, weighted by the inverse of the distance between each corner and the current point. This procedure is independent of the condensation level and ensures the maximum accuracy compatible with the accuracy of the original density. K and γ are adjustable parameters: their values were fixed at 2800 and 0.93, respectively, for E_{REP} in kJ mol^{-1}.

For a crystal, the total repulsion energy is a sum of two-body interactions

$$E_{REP} = 1/2\sum\sum E_{REP,AB} \tag{11}$$

where the factor 1/2 arises because of lattice sums (Appendix I).

V. Results and Discussion

The total intermolecular interaction energy is then

$$E_{TOT} = E_{COUL} + E_{POL} + E_{DISP} + E_{REP} \tag{12}$$

The adjustable parameters are ϵ_{max}, eq 3, D, eq 6, and K and γ, eq 9. An initial guess for their values was obtained through comparisons with results of ab initio calculations on dimers; the parameters were then adjusted by trial and error for the reproduction of sublimation energies in crystals (see below, section V.C). Appendix II collects the necessary numerical conversion factors.

A first strong point of this pixel−pixel formulation, in comparison with atom−atom ones, is that molecular electrical properties are distributed over an order of magnitude of 10^4 sites, rather than just a few nuclear positions, allowing a more accurate, flexible, and directional description of intermolecular forces. Even more important, the scheme includes penetration effects, or the effects of partial overlapping of molecular densities, as well as many-body effects in polarization energies.

A. Preliminary Tests. The total interaction energy in an argon dimer was calculated; a very smooth curve with a minimum of −1.4 kJ mol^{-1} at 3.6 Å was obtained, in agreement with experiment. To probe the effects of nonsphericity of the density, the calculation was repeated at a fixed distance of 3.2 Å, rotating the second electron density grid from 0 to 90° in steps of 15°. Coulombic, polarization, and dispersion energies stay constant, whereas the repulsion energy fluctuates between 11.8 and 12.4 kJ mol^{-1}.

In a benzene dimer, the distance between the two parallel and overlapping benzene rings was varied between 2.8 and 3.7 Å, and the calculation was repeated with the second ring rotated by 60° with respect to the first, to check the correspondence between molecular and electron density symmetry after condensation. Differences in repulsion energies were of the order of 1% or less; nevertheless, fluctuations in total energy of the order of a few kJ mol^{-1} were observed in this system at very short distances. They are probably to be ascribed to the systematic addition of small errors that occur when the grids of the two interacting electron densities are strictly parallel, and a very large number of identical distances (and hence of approximations in the same direction) are generated. In fact, the overall shape of the benzene−benzene interactions curve is smoother when one of the two densities is rotated by 60°.

B. Molecular Dimers. A few molecular dimers were studied: the acetic and formic acid cyclic dimers, the stacked, parallel-planes benzene dimer, and, for comparison with high-level, perturbation theory quantum mechanical results, the methyl chloride, acetonitrile, dimethylnitramine, methanol, formamide, and formamide−formaldehyde dimers. Numerical results are seen in Table 2. The acetonitrile and methanol dimer interaction data match surprisingly well those obtained from perturbation theory calculations. Agreement is good for the formamide and formamide−formaldehyde dimers, except for the repulsion energy in the latter. For the methyl chloride dimer, there is good agreement between IMPT and SCDS results for Coulombic and for repulsion energies, whereas dispersion and polarization energies are more stabilizing by our method, which thus results in a less repulsive total energy curve than IMPT. Overall, the agreement between CSDS results and quantum mechanical results is acceptable; considering that also QM results are sensitive to computational detail like basis set, etc., stretching further the parametrization to obtain a more strict correspondence was though both impracticable and scarcely useful.

The interaction curves for non-hydrogen bonding dimers are shown in Figure 1. They are similar to those obtained by quantum mechanics results.[13,14] For benzene, the Coulombic energy shows the expected small destabilization at about 3.5 Å, and the stabilization at short distances due to penetration effects. Incidentally, the point-charge representation of the Coulombic energy shows an unrealistic, steadily destabilizing trend (+10 kJ mol^{-1} at 3.2 Å, against a true value of −9.9 kJ mol^{-1}), a fact that, as already noted,[17] leads to many wrong interpretations of packing effects in organic crystals. Benzene is the most pathological case in what concerns energy fluctua-

TABLE 2: Interaction Energies[a] for Molecular Dimers

molecule	R_{min}[b]	E_{COUL}	E_{POL}	E_{DISP}	E_{REP}	E_{TOT}
methyl chloride, SCDS	(3.3)	−5	−3	−11	15	−4
methyl chloride, IMPT[13a]	(3.3)	−4	0	−4	13	5
formamide−formaldehyde, SCDS	2.00	−26	−10	−6	27	−16
	(1.88)	−33	−15	−6	44	−13
formamide−formaldehyde, IMPT[13b]	1.88	−35	−17[c]	−7	31	−27
acetonitrile, SCDS	3.46	−22	−6	−12	22	−19
acetonitrile, SAPT[14]	3.46	−26	−8	−17	26	−25
methanol, SCDS	4.1	−22	−5	−7	20	−15
methanol, SAPT[14]	4.13	−21	−6	−9	21	−15
formamide, SCDS	1.9	−78	−33	−15	84	−46
	(2.2)	−45	−12	−10	25	−43
formamide, IMPT[15]	2.17	−51	−13	−17	30	−51
formic acid, SCDS	1.7	−116	−63	−18	137	−67
formic acid, QM[16]	1.81					−58
acetic acid, SCDS	1.7	−118	−64	−19	139	−62
benzene, SCDS	3.2	−10	−10	−47	50	−17

[a] kJ mol^{-1}; IMPT and SAPT stand for intermolecular and symmetry-adapted perturbation theory, respectively. [b] Minimum energy separation: for acetic acid, formic acid, formamide and formamide-formaldehyde, O···H distance over the H-bond; for methyl chloride, Cl···Cl distance with C−Cl···Cl angle 90°; for the other dimers, distance between molecular centers of mass. In parentheses results for nonminimum energy separation. [c] Sum of induction and charge-transfer energies.

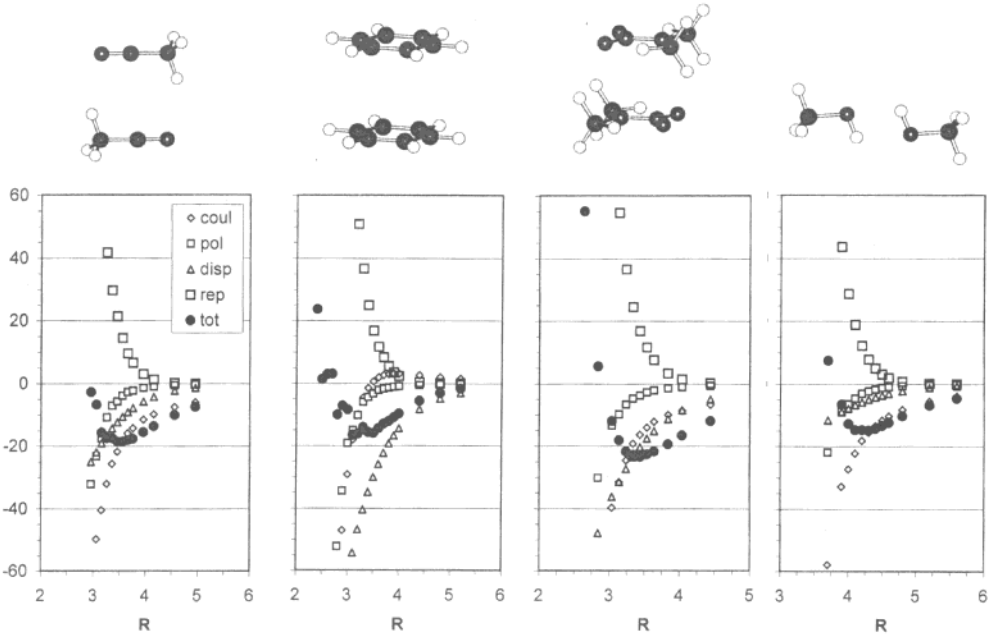

Figure 1. Energy curves (kJ mol^{-1}) in the (left to right) acetonitrile, benzene, dimethylnitramine, and methanol dimers. *R* (Å) is the distance between centers of mass.

tions in the short distance part of the curve. Figure 2 shows the interaction curves for the hydrogen-bonding dimers, where substantial overlap between electron densities appears: they are quite acceptable. All curves behave as expected as regards the position and depth of the energy minima and the asimptotic behavior at large separation. The calculated dimerization energy for acetic acid matches the experimental dimerization energy, 59−67 kJ mol^{-1}.[18]

In these dimer calculations, the relative importance of electrostatic and dispersion energies is coherent with interpretations based on molecular polarities and polarizabilities, whereas the role of polarization energy is seen to be important on an equal footing with the former two, more popular energy contributions. Energy fluctuations of the order of 1−5 kJ mol^{-1} because of numerical inaccuracies may be expected in the very worst cases at short molecular separations. Nevertheless, if one considers that the electron density is sampled at a step of 0.32 Å, the reliability of the energy calculation, performed in steps of 0.1−0.2 Å, is remarkable.

C. Crystals, Total Energies. Some organic crystal structures were chosen to match calculated total lattice energies with sublimation enthalpies or with the results of other methods for the calculation of intermolecular energies. The crystal model was constructed as described in ref 7, by repeating atomic coordinates and electron densities according to space-group symmetry and cell parameters obtained from the corresponding X-ray structure determinations. We assume that for our small and rigid molecules (with the possible exception of *n*-hexane) the contribution of molecular relaxation in the gas phase to the heat of sublimation is negligible.

A first test of the method concerns its response to changes in temperature; we used for this test a variable-temperature X-ray study of the succinic anhydride crystal.[19] Results are shown in Table 3: quite reasonably, at lower temperatures and higher densities, all stabilizing contributions become more stabilizing, whereas the repulsion energy rises correspondingly. From the net total energy change, an estimate of the contribution of potential energy to the sublimation ΔCp is obtained, about 10

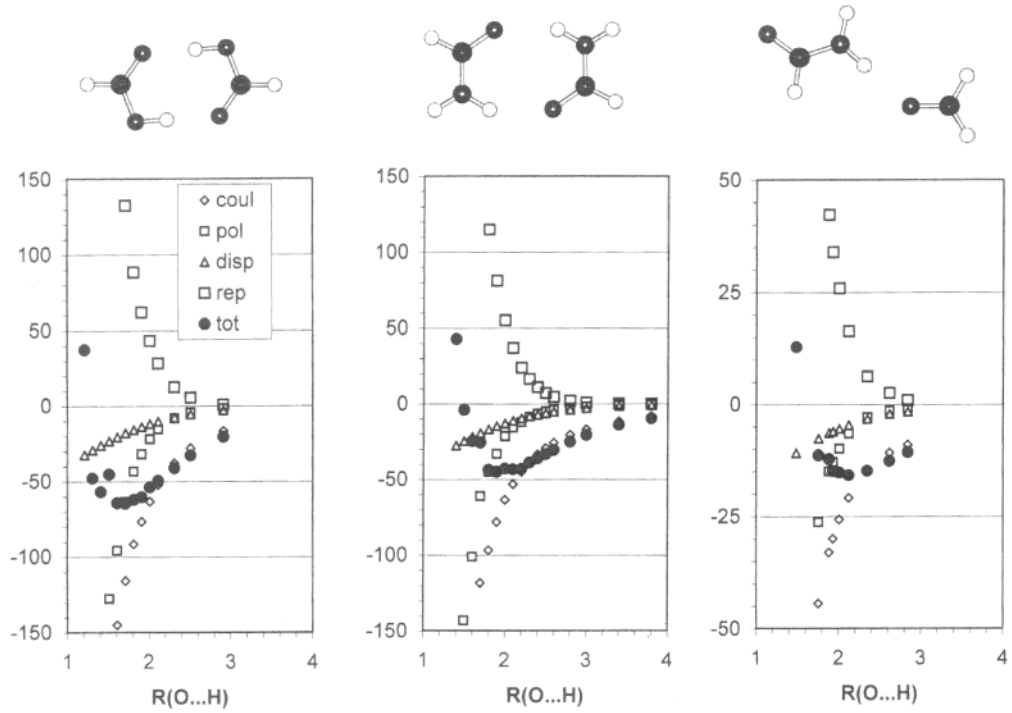

Figure 2. Energy curves (kJ mol^{-1}) in (left to right) formic acid, formamide, and formamide−formaldehyde dimers. *R* is in Å.

TABLE 3: Lattice Energies[a] in the Succinic Anhydride Crystal as a Function of the Temperature of the X-ray Crystal Structure Determination[b]

T/K	E_{COUL}	E_{POL}	E_{DISP}	E_{REP}	E_{TOT}	density/g cm^{-3}
100	−52.4	−15.8	−74.3	56.9	−85.6	1.575
150	−51.1	−15.2	−72.5	53.5	−85.3	1.559
225	−48.9	−14.2	−69.2	47.7	−84.6	1.531
295	−46.8	−13.3	−65.5	41.7	−84.0	1.499
353	−45.5	−12.7	−63.1	38.0	−83.2	1.478

[a] kJ mol^{-1}. [b] $n = 4$, cutoff at 15 Å.

J K^{-1} mol^{-1}, of the right order of magnitude. A more stringent test would be the complete relaxation of the crystal structure under the action of the potential field; this is so far impossible because of prohibitive computing times, but the lattice energy was evaluated (Figure 3) for an isotropic compression or expansion of the room-T cell dimensions. The minimum in the energy curve is quite acceptably located near the experimental structure, except for the usual moderate shrinkage that accompanies all calculations that neglect kinetic energies. One is impressed by the fact that total lattice energy variations result from a balance of wide variations in the four separate contributions, for such modest changes in intermolecular separations.

The results in Tables 4 and 5 show that calculated total lattice energies match sublimation enthalpies. For acetamide, the experimental value is rather high, if one compares with *N*-methylacetamide, whose crystal structure is however disordered.[29b] For pyrimidine, the experimental value is suspiciously lower than that for other azabenzenes (pyrazine 56.3, triazine 58.2 kJ mol^{-1};[33] see the discussion in ref 34a).

Coulombic, polarization, and dispersion energies change by only a few percent upon change in condensation level (repulsion energies stay constant by construction; the *K* and γ parameters should be slightly reoptimized for calculations with $n = 3$). Extension of the radius of the cutoff sphere from 12 to 15 Å has a marginal influence on Coulombic and polarization energies, as already noted,[7] and none on dispersion and repulsion, as expected from the inverse sixth power or exponential decay of these contributions.

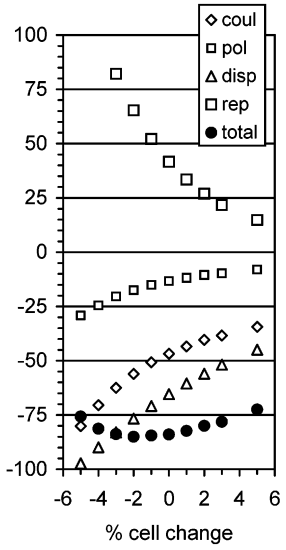

Figure 3. Energy contributions (kJ mol^{-1}) and total lattice energy in the succinic anhydride crystal for a simultaneous percent variation of the three cell edges.

For the formamide crystal, a distributed multipole calculation (the KP-ERP model of ref 35) is available, which includes Coulombic energies by a distributed dipole model, repulsion energies proportional to overlap, and dispersion energies using an empirical formulation. The energies are −56.1, +51.0, and −52.2 kJ mol^{-1}, respectively, to be compared with our values in Table 9. Our Coulombic energy is larger, as it includes the penetration energy; our dispersion energy is smaller, as it should, because the empirical formulation[35] presumably includes an unknown amount of polarization energy; and our repulsion is larger, because it has to counteract the highly stabilizing polarization and penetration energies. Thus, the comparison, which cannot be exact because of different approximations in the two methods, at least further demonstrates that our partitioned energies are of the right order of magnitude and behave

TABLE 4: Intermolecular Energies[a] in Non-Hydrogen-Bonding Crystals

crystal[b]	E_{COUL}	E_{POL}	E_{DISP}	E_{REP}	E_{TOT}	ΔH(subl)[33]
fcc argon	−0.9	−0.2	−13.8	5.4	−9.5	7.5
benzene[20]	−13.7	−5.4	−59.5	30.0	−48.6	44.4
	−12.4	−4.6	−59.2			
n-hexane[21]	−9.7	−3.8	−83.5	39.1	−57.9	50.6
succinic anhydride[19]	−46.8	−13.3	−65.4	41.6	−84.0	82.0
	−45.1	−12.8	−65.2			
1,4-benzoquinone[22]	−36.1	−9.6	−72.9	47.9	−70.6	68.6
	−34.7	−9.3	−72.5			
pyrimidine[23]	−28.6	−8.8	−61.3	39.5	−59.1	49.0
	−27.2	−8.2	−60.5			
1,4-dichlorobenzene	−25.5	−11.4	−98.9	63.2	−72.8	64.9
(γ phase)[24]	−23.0	−9.9	−98.4			
1,4-dinitrobenzene[25]	−38.6	−11.3	−93.7	53.9	−89.8	96.2
tetrathiafulvalene[26]	−43.9	−26.9	−115.6	96.6	−89.8	93.7
alloxan[27]	−96.7	−30.8	−103.4	113.1	−117.8	107−120[c]
	−92.5	−29.4	−104.0			

[a] kJ mol^{-1}. [b] First row: $n = 4$; second row: $n = 3$. [c] Estimated in ref 35.

TABLE 5: Intermolecular Energies[a] in Hydrogen-Bonding Crystals

crystal[b]	E_{COUL}	E_{POL}	E_{DISP}	E_{REP}	E_{TOT}	ΔH(subl)
formamide[28]	−79.8	−29.7	−38.2	87.0	−60.8	71.5
	−77.0	−28.3	−37.7			
N-methyl-	−57.8	−27.0	−47.9	75.6	−57.0	54.0
acetamide[29]	−56.7	−25.8	−47.6			
acetic acid[30]	−82.1	−46.4	−48.5	114.7	−62.3	67.4
	−78.9	−43.5	−48.0			
oxalic acid[31]	−117.0	−56.6	−71.8	140.5	−105.0	97.9
	−113.4	−54.3	−69.8			
benzoic acid[32]	−94.2	−55.1	−73.6	131.3	−91.6	89.1

[a] kJ mol^{-1}. [b] First row: $n = 4$; second row: $n = 3$.

as expected. This helps justifying our choice of the values for the four disposable parameters in our method.

D. Crystals, Molecule−Molecule Energies. Polarization energies are many-body ones and cannot be partitioned, but the present method allows an accurate partitioning of Coulombic, dispersion, and repulsion energies into molecule−molecule contributions. In a crystal, we define a symmetry cluster (also called a structure determinant[36]) as a subunit consisting of a reference molecule and *N* surrounding molecules; the parameters of a cluster are *R*, the distance between molecular centers of mass, *O*, the symmetry operator joining the molecules, and the repulsion, dispersion, and Coulombic energy contributions. $N = 1$ for a center of symmetry, $N = 2$ for translation, and $N = 2$ or 4 for a screw or a glide operator. For flat molecules, also an angle between molecular planes may be defined.

There certainly is a degree of arbitrariness in the partitioning of total intermolecular energies into polarization and dispersion ones, for example, and we are not oblivious of the limitations of some of our empirical assumptions. Nevertheless, our energy partitioning over molecules is unequivocal and as close to first principles as possible, challenged only by high-level quantum chemical calculations which at the present stage are unfeasible for full crystals. Therefore, an analysis of symmetry clusters allows a quantitative understanding of the relative importance of various kinds of energy in determining the structure of a crystal. Any partitioning over atoms would be much more arbitrary, and probably pointless; the concept of atom−atom bonding is proper in intramolecular valence arguments, but is improper in intermolecular interactions; there certainly is chemical bonding in crystals, but there are no easily identifiable intermolecular atom−atom bonds between different molecules, except perhaps for X−H···Y (X,Y = O,N) hydrogen bonds.

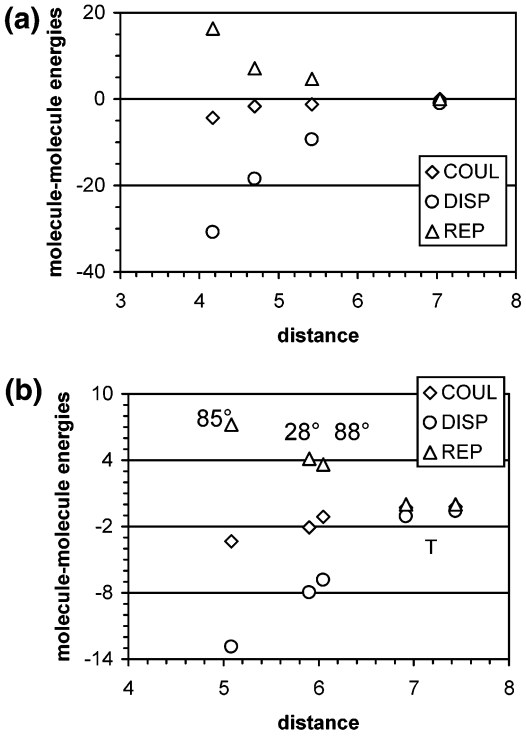

Figure 4. (a) Molecule−molecule energies (kJ mol^{-1}) in symmetry clusters, as a function of molecule-molecule distance (Å), in the *n*-hexane crystal. (b) The same in the benzene crystal. The interplanar angles are also shown. T denotes translation-related pairs.

The *n*-hexane crystal (Figure 4a) consists mainly of dispersive interactions between three molecular pairs related by pure translation, with aliphatic chains aligned side by side. The repulsion energy increases as dispersion energies become more and more stabilizing, but net cohesion arises because the dispersion energy is about twice the negative of repulsion. Contributions from Coulombic and polarization energies are negligible. In benzene (Figure 4b), the same pattern appears, and dispersion energy plays the main role even in the nearest-neighbor, so-called "T-shaped" molecular pair (85° interplanar angle), for which an explanation based on favorable Coulombic $H^{\delta+}...C^{\delta-}$ or quadrupolar interaction is usually invoked. Moreover, the three energy contributions are equal in the two next-neighbor clusters where the interplanar angle is 28° or 88°. Interestingly, the total molecule−molecule energies calculated by the present method are almost identical to those calculated by parametric atom−atom potentials,[34] as are the total lattice energies.

In benzoquinone, Figure 5, the picture is quite different. The closest neighbors (determinants A and B, Figure 6) interact mainly by dispersion, being essentially stacked parallel-planes arrangements, whereas next-nearest neighbors (clusters C and D, Figure 7) are edge-to-edge arrangements with significant Coulombic contributions from contacts between positively charged hydrogen zones and negatively charged oxygen zones. The case with pyrimidine (Figure 8) is somewhat perplexing: the by far dominating cluster is a 3.8 Å translation with stacked planes, where stabilizing interactions are of dispersive nature, counterbalanced by destabilizing repulsion and Coulombic interactions. Between 5.7 and 6 Å there are several clusters including a complex mixture of dispersion and Coulombic contributions with interplanar angles between 24 and 40°, not quite stacked, not quite T-shaped. One does wonder why the benzene crystal itself does not adopt the apparently so favorable 3.8 Å stacked planes arrangement found in pyrimidine, whose

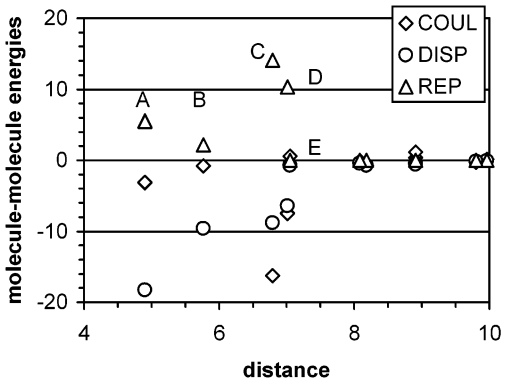

Figure 5. Molecule-molecule energies (kJ mol^{-1}) in symmetry clusters, as a function of molecule-molecule distance (Å), for the benzoquinone crystal. Symbols A, B, C, and D refer to the molecular arrangements shown in Figures 6 and 7. Cluster E is a stack of parallel molecular planes, which at 7 Å are too far away to interact significantly.

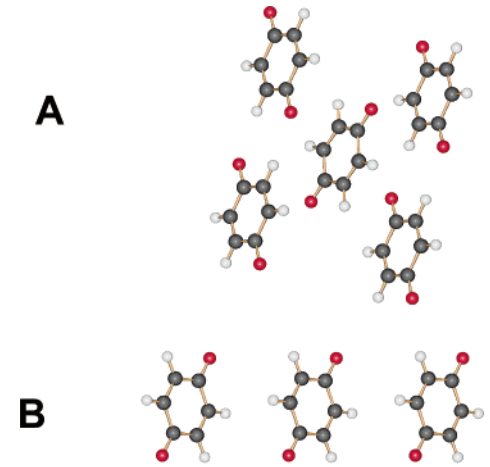

Figure 6. "Hydrophobic" (low Coulombic contribution) symmetry clusters in the benzoquinone crystal. A,B: see Figure 5. Graphics by SCHAKAL.[40]

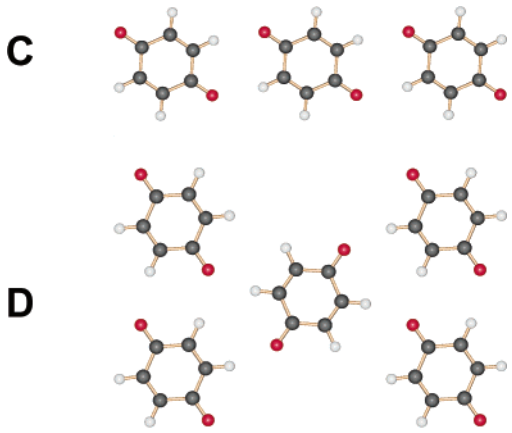

Figure 7. "Hydrophilic" (high Coulombic contribution) symmetry clusters in the benzoquinone crystal. C,D: see Figure 5. Graphics by SCHAKAL.[40]

energies are identical to those in the benzene dimer (Figure 1) at the same distance.

In the succinic anhydride crystal structure, one has (Figure 9) a set of first-neighbor clusters, Figure 10a, in which dispersion plays a role on an equal footing with Coulombic interactions, although the packing of this compound is usually explained in terms of "structure-driving" Coulombic C....O interactions. The Tx cluster (Figure 10b) is a good example of nearly perfect

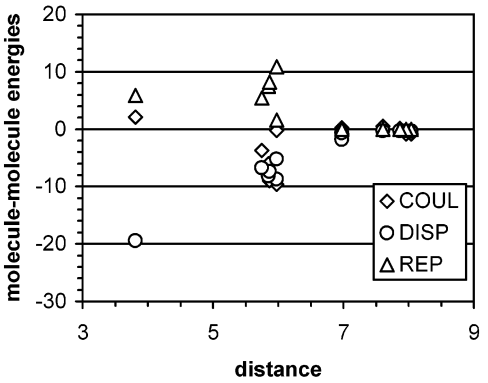

Figure 8. Molecule−molecule energies (kJ mol^{-1}) in symmetry clusters, as a function of molecule−molecule distance (Å), for the pyrimidine crystal.

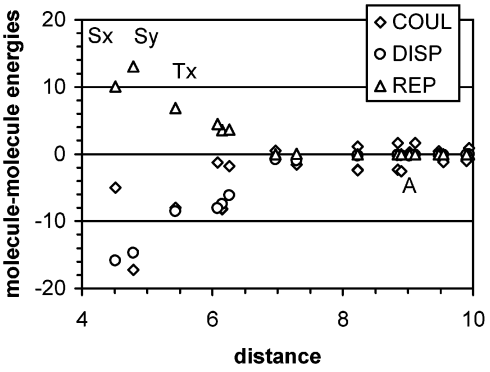

Figure 9. Molecule−molecule energies (kJ mol^{-1}) in symmetry clusters, as a function of molecule−molecule distance (Å), for the succinic anhydride crystal. The symbols denote arrangements shown in Figure 10.

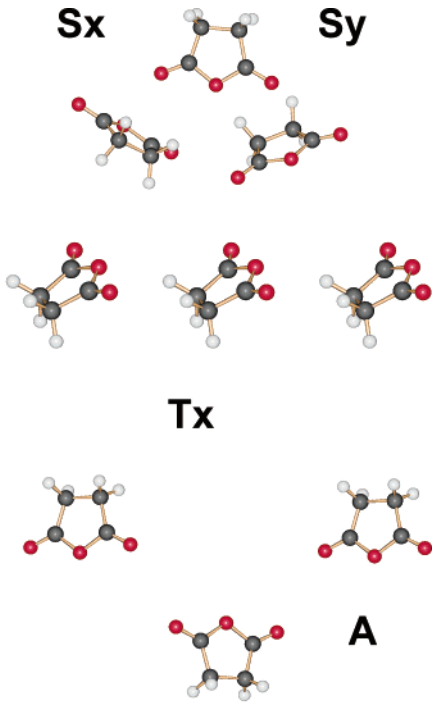

Figure 10. Molecular arrangements in three symmetry clusters for the succinic anhydride crystal; for the corresponding energies, see Figure 9. Graphics by SCHAKAL.[40]

juxtaposition between the hydrophobic and the hydrophilic parts of the molecule for best Coulombic interaction or even for what would be called C−H···O "hydrogen bonds", and yet, the

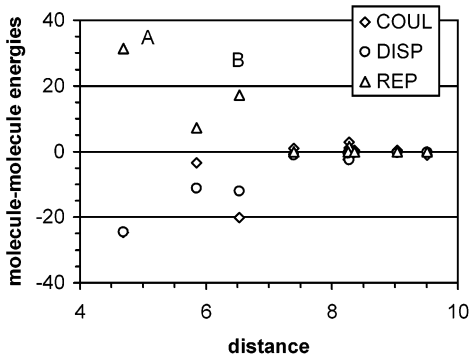

Figure 11. Molecule−molecule energies (kJ mol^{-1}) in symmetry clusters, as a function of molecule−molecule distance (Å), for the alloxan crystal. A,B: see Figure 12.

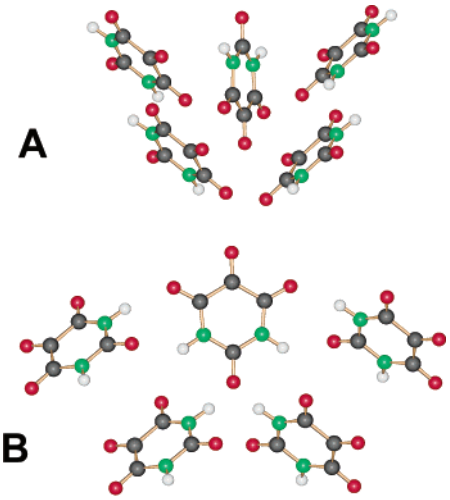

Figure 12. Molecular arrangements in the alloxan crystal structure, corresponding to energies shown in Figure 11. Graphics by SCHAKAL.[40]

TABLE 6: Molecule−Molecule Energies[a] in the Hydrogen-Bonding Pairs in Carboxylic Acid Crystals

crystal	E_{COUL}	E_{DISP}	E_{REP}	T/K	d(O···H)/Å
acetic acid	−72.2	−14.8	99.3	133	1.64
benzoic acid	−159.1	−15.7	191.6	room	1.62
oxalic acid	−44.5	−14.7	53.7	room	1.83

[a] kJ mol^{-1}.

dispersion energy is of the same magnitude as the Coulombic energy. Note a few destabilizing Coulombic terms between partners around $R = 9$ Å (one of them, labeled A, is shown in Figure 10c); these second-neighbor destabilizations are probably a price that has to be paid for the favorable first-neighbor interactions. Alloxan (Figure 11) solves its packing problem by forming a first-neighbor cluster (A, Figure 12) in which strong Coulombic and dispersion contributions coexist in the confrontation of oxygen-rich molecular peripheries and carbon-rich molecular cores, and this is probably one of the reasons why it does not need to form a hydrogen bond in its crystal. Incidentally, one would in vain try to sort out separate C···O interactions in the pictures in Figure 12.

The energy-distance diagrams for the carboxylic acids are not shown because the crystal structures invariably consist of just one highly predominant cluster formed by hydrogen-bonded partners, with very strong repulsion and Coulombic contributions. The Coulombic and repulsion energies in the cyclic dimer of benzoic acid (Table 6) are almost exactly twice the energies in each of the single hydrogen bonds in the acetic acid crystal; the energies in each of the single hydrogen bonds in oxalic acid

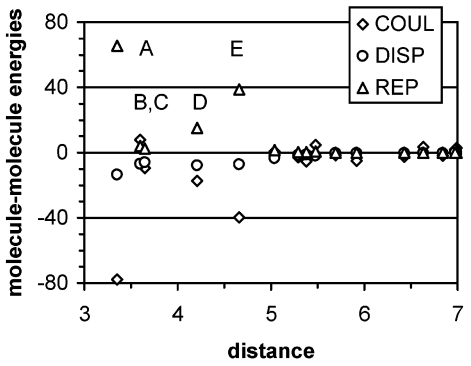

Figure 13. Molecule−molecule energies (kJ mol^{-1}) in symmetry clusters, as a function of molecule−molecule distance (Å), for the formamide crystal.

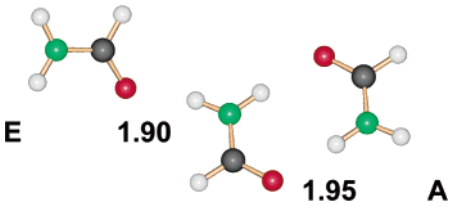

Figure 14. Hydrogen bonding arrangements in the formamide crystal. A,E: see Figure 13. Graphics by SCHAKAL.[40]

are much smaller, because the H-bonding distance is longer. Polarization energies are large in hydrogen-bonded systems, and this is not unreasonable if one remembers that our calculation is based on static, undeformed free-molecule electron densities.

In the formamide crystal (Figure 13), there are two hydrogen-bonding clusters, a cyclic one (A) over an inversion center, and a chain one (E) along a screw axis (Figure 14). The H-bond energies are quite similar, but in the E cluster, the repulsion and electrostatic energies are slightly larger than half those in the cyclic cluster, because in this last case the O···H distance is longer. The cluster denoted by D is a head-to-tail dimer over an inversion center with short O···H distances of 2.55 Å. Cluster B in Figure 13 corresponds to parallel molecular stacking along the x direction. Cluster C is an antiparallel stacked pair over an inversion center. The Coulombic energies are destabilizing and stabilizing, respectively, as in a simple dipole representation, but total energy contributions are almost negligible. One sees here a case of molecular proximity corresponding to insignificant intermolecular interactions, a further warning against the use of geometry arguments as a substitute for energetic arguments.

E. Concluding Remarks. We have presented a semiclassical, semiempirical method for the calculation of the main terms of intermolecular interaction energies, Coulombic, polarization, dispersion, and repulsion. With respect to rigorous methods for the calculation of intermolecular energies,[37] our approximations are, to say the least, brutal, and yet our results are in line with those of quantum mechanical models for dimers and reproduce the sublimation enthalpies of many crystal structures of organic compounds, at the cost of only four empirical parameters. The method requires only a readily available wave function, does away with cumbersome parametrizations, is readily applicable also by nonspecialists, and operates at a reduced computational cost: less than one to a few CPU hours on a modern workstation for one crystal structure, and just a few minutes for the interaction curves for dimers. Computing times are still prohibitive for application to large-scale structure search and optimization, or to molecular dynamics calculations. They may however become manageable in a few years time, also because so far no

special attention was paid to optimization of the program code with respect to running times.

The method is less accurate at very short intermolecular distances, where the interacting electron densities overlap considerably. This is not unexpected: static and undeformed free molecule electron densities are used, sampled at a rather large grid step, and the effect of core electrons on the overlap that determines the repulsion energy is neglected. Further refinements including a more efficient interpolation scheme are being presently considered.

Partitioning of total lattice energies into molecule−molecule contributions reveals how molecules interact in crystals and shows that geometry and intuition are not always good substitutes for energies. The partitioning of total crystal energies into their Coulombic, polarization, dispersion, and repulsion components reveals that total lattice energies are the sum of large contributions of opposite signs, all of which show substantial variations for small changes in geometry.

The method in its present form may not be accurate enough for a correct appreciation of the energy differences between polymorphs, and one wonders if any other presently available method is. A systematic test of the performance of the method in classifying polymorph crystal structures is under way.

Nevertheless, SCDS calculations allow a reliable distinction between Coulombic and dispersive interactions, for example. On the analytic side, information on the type and size of intermolecular energies is the key to a quantitative interpretation of intermolecular recognition phenomena and, eventually, of nucleation, growth, and molecular packing in crystals; on the synthetic side, that information offers a reliable guideline for the design of molecular aggregation on a quantitative basis. Quantitative aspects are vital in a field where energy differences are small, and conceptions based on electrostatics or vaguely defined steric and electronic effects are hardly applicable.

Acknowledgment. The author thanks Gerhard Raabe, J. D. Dunitz, and S. L. Price for useful discussions.

Supporting Information Available: Appendix IIIS and Table 7S, with computational details. This material is available free of charge via the Internet at http:/pubs.acs.org.

Appendix I. Corrigenda to Paper 1

In paper 1, results were quoted for MP2/6-31G** wave functions. Because of a factual mistake, for acetic acid, an HF/6-31G** wave function was used instead. None of the general conclusions are affected, but MP2 energies are proportional to the HF ones by factors of 0.97 for Coulombic energies, 0.74 for point-charge Coulombic energies, and 1.2 for polarization energies. Because of such a strict direct proportionality, the use of MP2 or HF densities does not change the general conclusions. The HF wave function was used also for hexachlorobenzene because of limitations in the quantum chemical program.

In paper 1, eq 12b, polarization energies resulting from lattice sums in crystals were multiplied by 1/2. This factor surely applies to all lattice sums over site−site terms, like Coulombic, dispersion, and repulsion energies, but does not apply to polarization energies, because A...B polarizations are different from B...A polarizations and hence there is no overcounting in the lattice sums. One should not confuse the 1/2 factor in the linear polarization formula, eq 1, with the lattice-sum factor (for more detail, see ref 38). Anyway, most conclusions reached in paper 1 using this wrongly applied factor were of a qualitative nature and, therefore, survive.

Appendix II. Conversion Factors

The computer program used for the calculations reported in the present paper (the computer code (about 2000 lines of standard FORTRAN) and input and output files for all of the calculations reported in this paper are available upon written request to the author. A fee may be applied for distribution of the computer code to profit organizations) uses as input distances in Å and charges in electrons, in conformity with chemical use. Further to the discussion of conversion factors given in paper 1, which left some ambiguities, the following is a list of factors for the conversion of results to SI units.

(a) Coulombic energies. The conversion factor is 1389.355 (two 1-electron charges 1 Å apart interact with an energy of 1389.355 kJ mol^{-1}).

(b) Electric field. The conversion factor is 1.439965×10^{11} (a 1-electron charge generates at a distance of 1 Å an electric field $\epsilon = 1.439965 \times 10^{11}$ V m^{-1}).

(c) Polarization energies. With volume polarizabilities in $Å^3$, and $E_{POL} = -1/2\ (4\pi\epsilon^\circ)\alpha\epsilon^2$, the overall conversion factor (in partial correction to footnote 12 of paper 1) is $8.60003 \times 10^{-18}/(4\pi\epsilon^\circ)^2$ or 694.676 (a 1-electron charge at a distance of 1 Å from a point with polarizability of 1 $4\pi\epsilon^\circ$ $Å^3$ units generates a polarization energy of −694.676 kJ mol^{-1}).

(d) Dispersion energies. Using mixed units of distances in Å, polarizabilities in $Å^3$, and the ionization potential in a.u. as it comes out of the MO calculation, the proper conversion factor is E_{DISP} (kJ mol^{-1}) = 1969.126 E_{DISP} (mixed units).

References and Notes

(1) Gavezzotti, A. *Synt. Lett.* **2002**, 201.
(2) Gavezzotti, A. *Modelling Simul. Mater. Sci. Eng.* **2002**, *10*, R1.
(3) Desiraju, G. R. *Angew. Chem., Int. Ed. Engl.* **1995**, *34*, 2327.
(4) (a) Hollingsworth, M. D. *Science* **2002**, *295*, 2410. (b) Aakeroy, C. B.; Beatty, A. M.; Leinen, D. S. *CrystEngComm* **2001**, *4*, 310 and references therein.
(5) Lommerse, J. P. M.; Motherwell W. D. S.; Ammon, H. L.; Dunitz, J. D.; Gavezzotti, A.; Hofmann, D. W. M.; Leusen, F. J. J.; Mooij, W. T. M.; Price, S. L.; Schweizer, B.; Schmidt, M. U.; van Eijck, B. P.; Verwer, P.; Williams D. E. *Acta Crystallogr.* **2000**, *B56*, 697.
(6) Motherwell, W. D. S.; Ammon, H. L.; Dunitz, J. D.; Dzyabchenko, A.; Erk, P.; Gavezzotti, A.; Hofmann, D. W. M.; Leusen, F. J. J.; Lommerse, J. P. M.; Mooij, W. T. M.; Price[j], S. L.; Scheraga, H.; Schweizer B.; Schmidt, M. U.; van Eijck, B. P.; Verwer, P.; Williams, D. E. *Acta Crystallogr.* **2002**, *B58*, 647.
(7) Paper I: Gavezzotti, A. *J. Phys. Chem.* **2002**, *B106*, 4145.
(8) Frisch, M. J.; Trucks, G. W.; Schlegel, H. B.; Scuseria, G. E.; Robb, M. A.; Cheeseman, J. R.; Zakrzewski, V. G.; Montgomery, J. A., Jr.; Stratmann, R. E.; Burant, J. C.; Dapprich, S.; Millam, J. M.; Daniels, A. D.; Kudin, K. N.; Strain, M. C.; Farkas, O.; Tomasi, J.; Barone, V.; Cossi, M.; Cammi, R.; Mennucci, B.; Pomelli, C.; Adamo, C.; Clifford, S.; Ochterski, J.; Petersson, G. A.; Ayala, P. Y.; Cui, Q.; Morokuma, K.; Malick, D. K.; Rabuck, A. D.; Raghavachari, K.; Foresman, J. B.; Cioslowski, J.; Ortiz, J. V.; Stefanov, B. B.; Liu, G.; Liashenko, A.; Piskorz, P.; Komaromi, I.; Gomperts, R.; Martin, R. L.; Fox, D. J.; Keith, T.; Al-Laham, M. A.; Peng, C. Y.; Nanayakkara, A.; Gonzalez, C.; Challacombe, M.; Gill, P. M. W.; Johnson, B. G.; Chen, W.; Wong, M. W.; Andres, J. L.; Head-Gordon, M.; Replogle, E. S.; Pople, J. A. *Gaussian 98*, revision A.7; Gaussian, Inc.: Pittsburgh, PA, 1998.
(9) (a) van Duijnen, P. T.; Swart, M. *J. Phys. Chem.* **1998**, *A102*, 2399. (b) Raabe, G.; Zobel, E.; Kock, R.; Souren, J. P. *Zeit. Naturforsch.* **1997**, *52a*, 665. (c) Miller, K. J. *J. Am. Chem. Soc.* **1990**, *112*, 8533. (d) Sum, A. K.; Sandler, S. I.; Bukowski, R.; Szalewicz, K. *J. Chem. Phys.* **2002**, *116*, 7627 and references therein.
(10) Rigby, M.; Smith, E. B.; Wakeham, W. A.; Maitland, G. C. *The Forces Between Molecules*; Clarendon Press: Oxford, 1986; p 34.
(11) Ling, M. S. H.; Rigby, M. *Mol. Phys.* **1984**, *51*, 855.
(12) See for example, Wheatley, R. J. *Chem. Phys. Lett.* **1998**, *294*, 487. Nobeli, I.; Price, S. L. *J. Phys. Chem.* **1999**, *103*, 6448.
(13) (a) Price, S. L.; Stone, A. J.; Lucas, J.; Rowland, R. S.; Thornley, A. E. *J. Am. Chem. Soc.* **1994**, *116*, 4910. (b) Mitchell, J. B. O.; Price, S. L. *J. Comput. Chem.* **1990**, *11*, 1217.
(14) Bukowski, R.; Szalewicz, K.; Chabalowski, C. F. *J. Phys. Chem. A* **1999**, *103*, 7322.
(15) Mitchell, J. B. O.; Price, S. L. *J. Phys. Chem. A* **2000**, *104*, 10958.

(16) Tsuzuki, S.; Uchimaru, T.; Matsumura, K.; Mikami, M.; Tanabe, K. *J. Chem. Phys*. **1999**, *110*, 11906.
(17) Dunitz, J. D.; Gavezzotti, A. *Helv. Chim. Acta* **2002**, *85*, 3949.
(18) See ref 34b for a discussion of this point.
(19) Ferretti, V.; Gilli, P.; Gavezzotti, A. *Chem. Eur. J*. **2002**, *8*, 1710.
(20) Jeffrey, G. A.; Ruble, J. R.; McMullan, R. K.; Pople, J. A. *Proc. R. Soc. London Ser. A* **1987**, *414*, 47.
(21) Nordman, N.; Mathisen, H. *Acta Chem. Scand*. **1961**, *15*, 1755.
(22) Trotter, J. *Acta Crystallogr*. **1960**, *13*, 86.
(23) Wheatley, P. J. *Acta Crystallogr*. **1960**, *13*, 80.
(24) Wheeler, G. L.; Colson, S. D. *J. Chem. Phys*. **1976**, *65*, 1227.
(25) Di Rienzo, F.; Domenicano, A.; Riva di san Severino, L. *Acta Crystallogr*. **1980**, *B36*, 586.
(26) Cooper, W. F.; Edmonds, J. W.; Wudl, F.; Coppens, P. *Cryst. Struct. Commun*. **1979**, *3*, 23.
(27) Swaminathan, S.; Craven, B. M.; McMullan, R. K. *Acta Crystallogr*. **1985**, *B41*, 113.
(28) Stevens, E. D. *Acta Crystallogr*. **1978**, *B34*, 544.
(29) (a) Katz, J. L.; Post, B. *Acta Crystallogr*. **1960**, *13*, 624. (b) Hanzaoui, F.; Baert, F. *Acta Crystallogr*. **1994**, *C50*, 757.
(30) Jonsson, P.-G. *Acta Crystallogr. B* **1971**, *27*, 893.
(31) Derissen, J. L.; Smit, P. H. *Acta Crystallogr*. **1974**, *B30*, 2240.
(32) Sim, G. A.; Robertson, J. M.; Goodwin, T. H. *Acta Crystallogr*. **1955**, *8*, 157.
(33) Chickos, J. S. In *Molecular Structure and Energetics*; Liebman, J. F., Greenberg, A., Eds.; VCH: New York, 1987; Vol. 2.
(34) (a) Filippini, G.; Gavezzotti, A. *Acta Crystallogr*. **1993**, *B49*, 868. (b) Gavezzotti, A.; Filippini, G. *J. Phys. Chem*. **1994**, *98*, 4831.
(35) Coombes, D. S.; Nagi, G. K.; Price, S. L. *Chem. Phys. Lett*. **1997**, *265*, 532.
(36) Gavezzotti, A.; Filippini, G. *J. Am. Chem. Soc*. **1995**, *117*, 12299.
(37) Stone, A. J. *The Theory of Intermolecular Forces*; Clarendon Press: Oxford, 2000.
(38) van Eijck, B. P.; Kroon-Batenburg, L.-M−J-; Kroon, J. In *Theoretical Aspects and Computer Modeling of the Molecular Solid State*; Gavezzotti, A., Ed.; Wiley: Chichester, U.K., 1997; Chapter 4, pp 130−132.
(39) Rowland, R. S.; Taylor, R. *J. Phys. Chem*. **1996**, *100*, 7384.
(40) Keller, E. SCHAKAL92, *A Program for the Graphic Representation of Molecular and Crystallographic Models*; University of Freiburg: 1993.